Thermal Behaviour of a V-MCM Package Containing a Thermo-Pneumatic MicroPump, Sensors and Integrated Electronics

J. Sieiro[1], A. Morrissey[2], M. Carmona[1], S. Marco[1], J. Samitier[1], J. Alderman[2]

[1]Departament d'Electrònica, associated unit to the CNM-CSIC, Universitat de Barcelona,
Av. Diagonal 645-647, 08028-Barcelona, Spain. santi@el.ub.es
[2]NMRC, University College,
Lee Maltings, Prospect Row, Cork, Ireland. amorisey@nmrc.ucc.ie

ABSTRACT

This paper describes the thermal behaviour of vertical multichip module (V-MCM) devised within the BARMINT Esprit Project. It encloses an stack of elements including several ICs, a micromachined pump, and a multisensor chip provided with pressure sensors, ISFETs and temperature sensors together with signal conditioning circuitry. All these elements are embedded in a 3D cube made of PLCC (Plastic Leadless Chip Carriers).

I. INTRODUCTION

This paper is based on work performed in the Esprit 8173 project BARMINT (Basic Research for Microsystems Integration), where one of the requirements is to investigate the problems associated with 3D packaging a microsystem with biomedical applications. The BARMINT microsystem includes a sensor chip fabricated at CNM (Spain), which carries ISFET-based chemical sensors, piezoresistive pressure sensors and temperature sensors. Integrated in the same chip, there is also signal conditioning circuitry for all these sensors and one analog multiplexer, all in CMOS technology. Within the same package, there is also a micropump module fabricated at LAAS (France), shown in Figure 1, which carries fluids to the sensor chip for analysis. The pump construction also includes delicate micromachined microvalves to control the direction of fluid flow. The packaging has to allow for the need for inlet / outlet tubes, as well as a reference pressure inlet port on the side of the cube at the level of the sensor chip. These features and requirements will become apparent in later text and diagrams. Detailed discussions on the operation of the pump are available elsewhere [1-2]. Power supply and signal processing modules complete the microsystem. They are stacked below the pump and sensor modules.

In this work several issues concerning the package of this highly complex microsystem will be discussed. The thermal behaviour of the V-MCM developed within the project will be studied. This is a key point since the package includes thermally based actuators, namely, a thermo-pneumatic micropump which dissipates a non-negligible amount of power (1 W). This value is comparable to the total dissipation of a 256 Mbit DRAM module. The thermal performance of the V-MCM is critical due to the low thermal conductivity of the plastic compounds used.

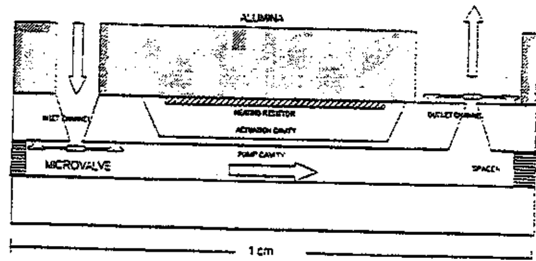

Fig. 1 Cross-sectional scheme of the micropump

The understanding of the thermal behaviour answers several questions: which will be the operating temperature of the electronics, how the performance of the thermo-pneumatic micropump will be affected by the package and different boundary conditions, which will be the temperature increase in the pumped fluid. In addition thermal simulations are essential for the analysis of thermal stresses which can be very important due to the presence of delicate micromechanical structures.

On the other hand, there is an important point that differenciates the present study from previous thermal studies of MCM. In more conventional high power density packages, the main objective is the reduction of the total thermal resistance of the package, to reduce the operating temperature of the electronics. However, in our case one of the components of the assembly, the pneumatic pump needs to be operated at a certain temperature for internal pressure build up. Hence, we do not look for very low thermal resitance from the micropump heater to the ambient. Moreover, while in most applications DC behaviour is the only concern, in the thermal analysis presented in this paper special emphasis is given to the study of transient behaviour because of the pulsed mode of operation of the pump.

Section II is devoted to the problems which appear in microsystems packaging. Section III describes the particular package solution adopted by NMRC in the BARMINT project. Section IV describes how we approached the thermal simulation: which problems we encountered and how we solved them. Section V focus on the static and dynamic simulation results while analyzing which lessons can be extracted concerning the design of efficient packaged microsystems. Section VI summarizes the main conclusions of this work.

II. PACKAGING ISSUES OF MICROSYSTEMS

Encapsulation of the Microsystem in plastic allows it to be packaged and lends itself to high volume production, but because of TCE mismatch between different materials within the Microsystem, the packaging process may generate high levels of stress which can negatively affect the system's operation and reliability. Indeed, the mismatch between the mechanical properties of the materials is one of the most critical issues governing the reliability of electronic packaging. Encapsulation results in large residual stress of the order of 1 Ton/cm^2 which poses severe problems for conventional packaging [3]. Residual stress is often a function of temperature so that sensors designed to operate in thermally changing environments need to be designed to operate over a range of stress values. In selecting package materials for moisture protection, adhesion of the encapsulant is as important as the permeability. Loss of adhesion leads to dramatic altering of the internal stress state [3] often resulting in cracking of the chip and / or plastic and rapid progression of delamination over material interfaces. A delamination provides a simple route for moisture ingress. Encapsulation processes need to be optimised and the recipes for encapsulants need to be improved to minimise the risk of delaminations. One of the main goals of IC packaging is to keep moisture out of packages. A fluid analysis microsystem may need to take fluid into the package, a concept alien to IC package designers.

3-D packaging techniques have great potential for microsystem integration. 2-D packaging is not suitable for the advanced packaging densities required by the Space agencies [4]. It is necessary to go down the MCM route or follow some 3-D packaging scheme of which there are many. The 3-D MCM-V packaging technique proposed by Val [5] achieved memory densities never seen before. Encapsulated in plastic, it had a very low mass making it ideal for Space applications. Proper thermal management of 3-D packages is more crucial than for 2-D packages [4]. Unlike 2-D approaches which can rely on sufficient "package surface cooling area" for each die, 3-D packages with multiple die depend almost totally on advances in materials to remove heat from internal layers. A commonly used rule of thumb for standard ICs is that the lifetime of a device is halved for every 10°C temperature rise above an operating temperature of 125°C [6]. Microsystems often require miniaturised packages and consequently very small die size, particularly in medical applications. While decreasing die size may give more die per wafer, yield problems could result from dicing and handling the small die.

III. 3D PACKAGING OF THE BARMINT ASSEMBLY

Previous approaches to the production of the BARMINT demonstrator have included the encapsulated stacked silicon preforms method [7], whereby chips are mounted and wirebonded on silicon preform substrates. These are stacked in a mould which is then filled with epoxy. After curing of the epoxy, the final shape is obtained by sawing through the wirebonds to cut out the central section. Due to TCE mismatch between silicon and the encapsulant material, delaminations of the stacked units can occur, and due to the geometry and shape of the cutting window (in addition to the TCE mismatch issue) there is a large concentration of stress at the cutting window. Reference [6] proposed a modified design of the cutting window in order to reduce this stress. The NMRC also proposed [8] a "Board and Spacer" approach based on PCB substrates, with COBs spaced by slices of PCB in a 3D stack. Again, the final shape resulted from sawing, grinding and polishing steps. Herein, a different approach is described. It is based on an assembly technique using standard off-the-shelf components.

The PLCC Approach

Alignment issues and reproducibility of identical-sized boards were limiting factors in the board and spacer approach. An alternative method was sought. The use of a commercially available standard-sized plastic leadless chip carrier (PLCC) is a cheaper option than the procurement of custom made board and spacer units, particularly when the tolerances involved mean higher costs if the track misalignment problem [8] is to be eliminated. Even then it is extremely difficult to maintain the parts in position during assembly and curing. This problem is eliminated in the PLCC approach illustrated in Figures 2 and 3.

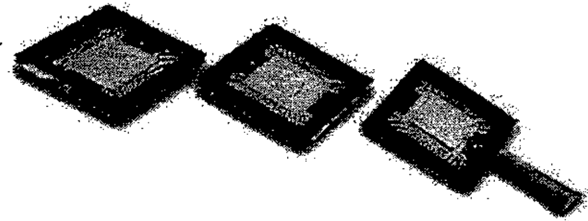

Fig. 2 Plastic Leadless Chip Carrier

Figure 2 shows a typical PLCC. The PLCC is a chip carrier containing a cavity with walls constructed from PCB-type material. The chip sits on a die paddle in the centre of the carrier and is held in place with a die attach material. With large die or stress sensitive die, stresses caused by TCE mismatches between silicon and the substrate board become evident once the cured (and now solid) adhesive cools to room temperature. Greater contraction of the substrate relative to the silicon chip produces a thermal stress which can easily damage the chip. A material was chosen which has a large radius of curvature upon curing, and which cures at a relatively low temperature of 125°C. The use of flexible adhesive films instead of epoxy paste adhesives was found to be unsuitable for two reasons, viz. ease of handling and the need to apply a pressure during application and curing; the latter point is particularly undesirable when micromachined silicon membranes were involved in the die in question. The bond pads on the chip are wirebonded to tracks on the board. The wirebond loop height must be lower than the height of the surrounding walls to avoid damage from the chip carrier on the next level. There is no need to glue spacers to vertically separate the individual die because the cavity in which the chip is placed is part of the package structure. In addition to reducing the number of process steps, it also results in better sealing and package integrity.

The cavity is filled with a glob-top material. A range of encapsulating materials were evaluated for suitability. In particular, the recommendation of the previous study [8] to use soft materials was implemented. Both heat-curing and UV-curing silicone gels were investigated. In light of the fact that the use of low temperature curing glob-tops is a means of further minimising the associated stresses, a particularly suitable gel is one which cures at room temperature. The gel used is also very resistant to chemicals and moisture, with excellent electrical insulation properties, obviously important considerations for the encapsulation of chips in a microsystem intended for sensory applications.

The assembly process is repeated for all of the components of the BARMINT microsystem apart from the micropump and sensor chip modules at the top of the stack. This is described separately below.

Packaging of the Micropump and Sensor Chips

The sensor chip is die attached to the chip carrier in a conventional manner and wirebonded out to the board. For the purposes of protecting these wirebonds, the same silicone gel as mentioned previously is dispensed around the periphery of the chip, encapsulating bondpads and wirebonds but leaving the central sensor area free of silicone gel. The micropump module is attached to a second PLCC by means of conductive epoxy adhesive to the alumina heater side of the component. The PLCC is then inverted and attached to the PLCC carrying the sensor chip by means of the same adhesive used to glue the MCM units together in the 3D assembly. The sensing chamber construction is completed by means of a polysiloxane square-ring gasket between the pump and sensor chips. The thickness of the polysiloxane determines the volume of the pumping chamber beneath the membrane. It also acts as a seal to prevent fluid leakage. It is put in place prior to gluing the chip carriers together. The use of photolithographic deposition of organic membranes such as polysiloxane has been demonstrated in applications, as a gas permeable membrane covering an ISFET or CHEMFET [9], and in 3D assembly by the researchers at Neuchatel[10]. It is a chemically and physically stable silicone rubber which undergoes small changes in elastic modulus with temperature (1.1 kPa/°C). It is both highly compressible and very flexible making it ideal for this application. The inlet /outlet system is put in place by drilling holes in the chip carrier to which the

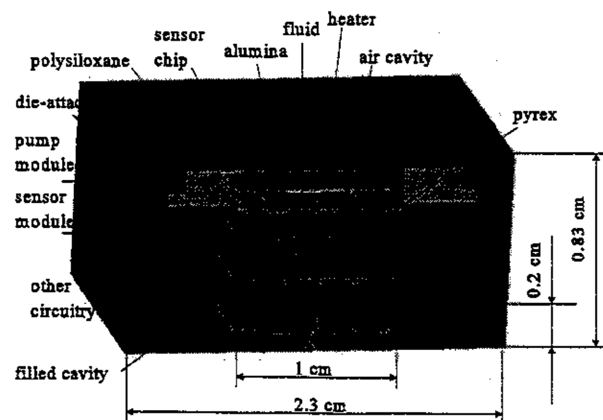

Fig. 3: The PLCC Approach

pump unit is attached. Fluid is supplied to the pump and removed by tubes as illustrated in Figure 4. The tubes used are 1.6mm outer diameter sections of pique tubing and are set in place using an epoxy. With pressure sensors, there is a need for a reference pressure inlet port. The sensor chip is

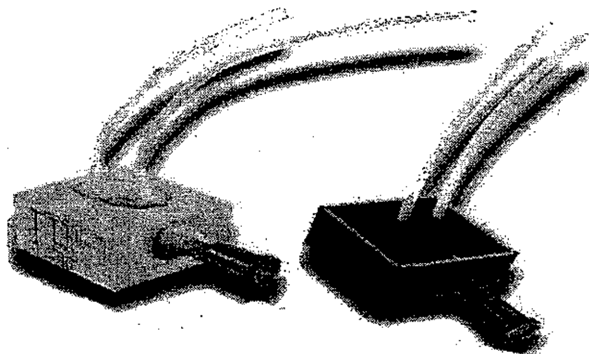

Fig. 4 Photograph of fabricated BARMINT demostrator.

comprised of a 300mm thick silicon chip bonded to a 1mm thick glass chip. The latter has a 600mm wide groove. Once this chip is die attached to the chip carrier, a hole is drilled in the side of the carrier and a needle is placed through this and into the groove in the glass as shown in Figure 2. The needle is secured in position by using epoxy at the point of entry to the carrier wall as illustrated in Figure 4. Simple tests have shown this system can withstand pressures of at least 3 Atm, which is greater than the requirements of the BARMINT project.

To produce the final stack, the adhesive used for the assembly of the modules was selected on the basis of a number of criteria :

i) good bonding, with no evidence of delaminations after 1000 temperature cycles between -55°C to + 125°C with a dwell time of 10 minutes at each extreme
ii) purity level
iii) ease of handling
iv) screen printability (with a view to bulk manufacturability)
v) safety
vi) resistance to plating chemicals
vii) adhesion of the Cu / Ni / Au plated metallisation.

The PLCCs are held in place during the curing of this adhesive using a clamping apparatus which is capable of simultaneously exerting a side-on and downward force. Thus the alignment of the stacked carriers is maintained while also providing the clamping pressure necessary to guarantee a uniform and void free joint between each level after curing has been completed. A further improvement over the previous board and spacer approach is the elimination of the sawing step [8]. While the stresses associated with sawing are minimal in the board and spacer approach, they are eliminated completely in the current method. The obvious additional benefit of eliminating a process step is reduced fabrication time, and thus cost.

Interconnection

The outer surfaces of the cubic blocks are plated with a layer of electroless copper, followed by a barrier layer of electrolessly deposited nickel. Plating solutions developed at NMRC were used in these steps. Electroless plating is the controlled autocatalytic deposition of a metal film by the interaction in solution of a metal salt and a reducing agent. Once the copper and nickel layers are in place, the finish is provided by immersion plating from a commercially available gold bath. The nickel layer prevents copper ions from electromigrating through the relatively soft gold layer Immersion plating differs from electroless plating in that it is not autocatalytic, i.e. only a definite thickness will be deposited irrespective of plating time. The gold finish was chosen not just because of its electrical properties but also because of the inertness of gold metal. An Argon-Fluoride excimer laser at NMRC is used to write the required interconnection pattern on the relevant faces of the cube. Figure 4 shows a photograph of two 3D assemblies with the inlet and outlet tubes in place in addition to the reference pressure inlet ports. The sample on the left has been plated with Cu / Ni / Au and a sample pattern has been laser-written on one side.

IV. MODELLING PROBLEMS AND SOLUTION PROCEDURE

At this point the reader will have probably grasped the complexity not only of the microsystem but also the package itself. An axiom of 'modelling art' is that you have better not to start modelling the problem in the maximum level of detail. A side consideration is that modelling simplifications are always a need. Plausible hypothesis have to be issued and the engineer has to proceed from rough models to more accurate ones.

When modelling a system like this, the temptation can be to develop a high complex 3D model of the system. However the increased simulation accuracy which can be extracted from this effort is hidden because of the following considerations:

i) Material properties are not well known. This is a recurrent problem in microsystems FEM simulations because of the continuous experiences with novel materials.

ii) High-aspect ratio structures typical in microsystems will force to use a very fine mesh, which could not be practical.

Taking into account these considerations one has to be realistic when stating the expected predictive capabilities of the analysis. In most cases models show very good qualitative agreement but deceptive quantitative results.

Because of the above considerations we adopted as modelling strategy the development of a 2D axisymmetric model. The biggest advantatge is that the time to develop the model and the CPU simulation time is greatly reduced. Our physical model has almost a 4th order symmetry axis which passes through the center of the model from top to bottom. This axisymmetric approach has been previously used by Hall[11] and Darveaux[12]. In agreement with their procedure, we have decided to treat the V-MCM as a cilinder with an effective radious of $L/\sqrt{\pi}$ (where L is the edge length of the assembly perpendicular to the symmetry axis). This approach equals the areas perpendiculars to the axis. Although we believe this is a good approximation, it understimates the heat flow to the ambient in perpendicular direction to the symmetry axis. In addition, electrical contacts, reference pressure channel, pressure sensors and fluid connections are elements which distort slightly this symmetry.

A cross-section scheme of the model can be observed in Figure 3. Note the presence of very different materials: alumina, silicon, chip carriers, filling materials, die attachs, pyrex, etc. The material properties used for the simulation are presented in Table I.

Now we will discuss several details of interest in our model including the different mechanisms of heat loss. We have estimated that less than a 10% of the total power is going to

Table I: Material Properties for simulation.

Material	K erg/(cm.s.°C)	C erg /(g·°C)	Dens g /cm^3
Chip Carrier(CC)	$5 \cdot 10^4$	$1.25 \cdot 10^7$	1.1
Filling material	$1.8 \cdot 10^4$	$1.03 \cdot 10^7$	1.04
CC Adhesive	$4 \cdot 10^4$	$0.3 \cdot 10^7$	1.4
Die-attach glue	$2.5 \cdot 10^5$	$0.418 \cdot 10^7$	3.3
Silicon	$1.56 \cdot 10^7$	$7.13 \cdot 10^6$	2.329
Pyrex	$1.09 \cdot 10^5$	$0.84 \cdot 10^7$	2.24
Air*	$2.6\text{-}3.95 \cdot 10^3$	$1 \cdot 10^7$	10^{-3}
Polysiloxane	$0.5 \cdot 10^5$	$1.2 \cdot 10^7$	1.5
Fluid	$0.588 \cdot 10^5$	$4.18 \cdot 10^7$	1
Pump Adhesive	$2.4 \cdot 10^5$	$0.6 \cdot 10^7$	1.5
Elect. Insulator	$0.6 \cdot 10^5$	$0.85 \cdot 10^7$	1.71
Metals	$3 \cdot 10^7$	$0.71 \cdot 10^3$	3
Alumina	$3 \cdot 10^6$	$8.73 \cdot 10^6$	3.78

*Air density dependence on temperature has been considered

escape through the electrical contacts. This heat loss path has been modeled as a thermal bar directly connected to the heating resistor. A back of the envelope calculation has also proved that for the expected flows, the amount of heat expelled by the pumped fluid is negligible. Because the chip carrier has a low thermal conductivity, we expect that the temperature in the external surface of the package will be low. As a consequence, we have decided not to include radiation losses in the model.

Due to the final expected application of the demonstrator two different boundary conditions have been selected: surrounded by air and surrounded by water (in vivo implantation). We would like to put into evidence that we would like to simulate not just test conditions but more realistic working conditions. The thermal resistances in real operation conditions tend to be quite different from those obtained when the device is located in a thermal test system[13]. The total heat transfer coefficient has been obtained from the comparison between thermal simulations and thermography images obtained by the Technical University of Lodz (a BARMINT partner) with similar devices. The values taken have been:

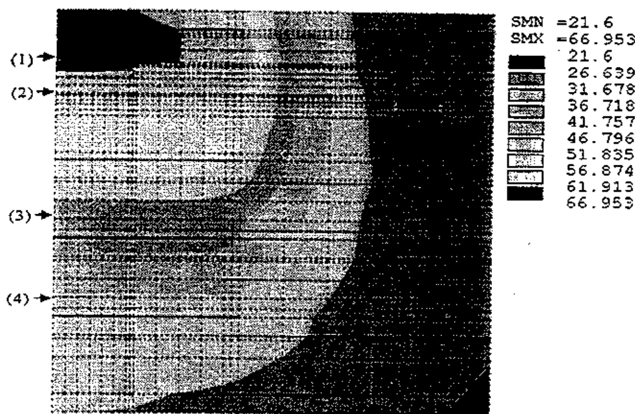

Fig. 5 Static temperature distribution when in air. (1W)

h_{air}=4.10^{-3} W/(Kcm^2) , h_{water}=4.5.10^{-2} W/(Kcm^2) . They summarize the conduction and convetion losses to the ambient.

Very thin (compared to the total package size) metal layers in the base of the PLCCs have been treated as 2D elements because of prohibitive aspect ratio, and negligible temperature gradient perpendicular to the layer. Multilayers composites have been replaced by an equivalent element whose properties are obtained by weighting the properties of the compounds according with the expected direction of the heatd flow.

V. STATIC AND DYNAMIC RESULTS

The results of the simulation are shown in Figure 5. The plots show the temperature distribution within the module. The results are shown for an ambient temperature of 21°C with natural convection in the surface (symmetry axis is adiabatic). Two boundary conditions are considered: heat exchage coefficients representing the inmersion in air or water. 1W continuous power was applied to the heating resistor in the micropump. Of course, in both simulations the heater is the hottest point in the structure, with a high temperature region in the alumina substrate where the heater is located. The thermal resistance is 43.5°C/W when in air, and 19.4°C/W when in water. This result can be directly attributed to the augmented heat exchange coefficient in the second case. This value can be compared with junction-to-ambient thermal resistance values of 88-104°C/W obtained in the TRIMOD project[14]. This relative low thermal-resistance can be due to the enlarged exterior surface area, which diminishes the contribution of the case-to-ambient resistance. While in the TRIMOD project the sizes of the cube where about 10x10x15 mm in the case the cube is a little bit larger (see figure 3).

From the temperature plot several more conclusions can be drawn. Considering first the boundary conditions in air: the temperature of the water is about 50°C, almost equal to the temperature in the sensor chip. This point will have to be considered when designing the electronics in these chips. Specially as regards to sensor temperature cross-sensitivity compensation. Fortunately, this chip includes several temperature sensors which can provide a valuable signal for this compensation. Moreover no significative temperature

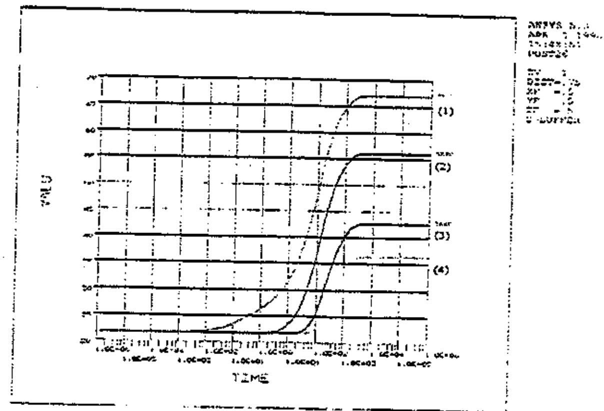

Fig. 6 Temperature evolution in different point of the package (see figure 5).

differences appear along every single chip. This is a expected result becuase of the high thermal conductivity of silicon. The rest of the electronics will suffer also the influence of the pump, although the temperatures are lower. In this sense, the pyrex support of the sensor chip, due to its low thermal conductivity isolates a little bit the rest of the electronics from the pump. Because of the same considerations, a suggestion for better isolation is not to fill completely every PLCC cavity, but only the necessary, letting an air gap to the PLCC above. This will isolate better the electronics from the pump without increasing too much the total thermal resistance seen by the heater, because most of the flux goes to the exterior through the upper part of the package. A second consideration is the low temperatures of the exterior surface, except the upper surface. This result supports the hypothes of neglecting radiation losses. When the exterior of the package is water, similar conclusions can be drawn althoug all the temperatures are lower. Temperature in the flowing fluid is about 34°C and 32°C in the sensor chip.

From the flux diagrams there is an important phenomenon to note: most of the heat flux goes directly into the alumina, instead of flowing inside the air cavity. This point affects dramatically the dynamic response as we will see soon.

As the operation mode of the micropump relies on pulsed power supply, it is very important to look at the dynamic behaviour of the system. Simulation has shown that the dynamics of the structure are very slow (Figure 6). To obtain significative temperature excursions, the frequency of the power signal has been decreased up to 0.01 Hz. For this pumping frequencies the flow will be too small. This is true whatever the boundary conditions we choose. In water the response is faster but at the expense of a reduced temperature range variation.

From this results, we studied an alternative design with a suspended heater. In this design a small silicon plate containing the heater and supported by four small beams. In this way, a higher thermal resistance from the heater to the rest of the package is achieved. Higher temperature excursions occur. Moreover by virtue of the smaller thermal mass a very fast response is achieved (figure 7). Only the heater and the surrounding air in the pumping cavity achieve high temperatures while the rest of the package remains at a

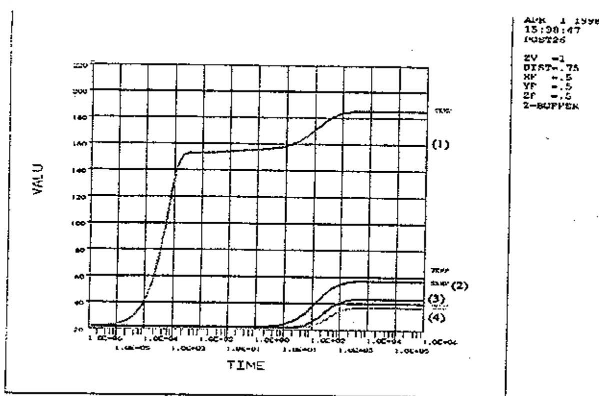

Fig. 7 Temperature evolution in the same points with a hanging resistor design.

lower temperature. Maximum isolation is achieved with this design. Looking at the transient diagram we may observe that for frequencies of 100 Hz a temperature excursion in the heater of 120°C is feasible and the package does not respond until times of the order of 100s.

VI. CONCLUSIONS

To compare the presently described approaches for the packaging of the BARMINT demonstrator with the TRIMOD method [14], there are points which illustrate that it is better to use preforms. Using preforms, the final shape is already there, defined without a need to cut out the shape at the end of the process, as was necessary in TRIMOD. With the latter, the final cube had to be sawn out and manipulated. Also, from a yield increase viewpoint (and hence cost reduction), BARMINT as described in this paper is an assembly of pre-testable modules and only working modules are included in the final stack and those which fail can be eliminated without their giving rise to a failure in a 3D assembly which may carry up to 5 such modules in all.

In BARMINT, by attempting an extremely difficult task in assembling such a wide variety of pieces, from various technologies, a lot of problems were encountered and in most cases solutions were found and are suggested in this paper, such that the project served a useful purpose as a troubleshooting exercise in 3D packaging of microsystems.

Concerning modelling, we have studied the thermal performances of the system using a 2D axisymmetric model. This model has proven to be a useful tool in the study of the thermal behaviour. Important infomations have been drawn concerning the working temperatures of the different electronic chips. Perhaps, the most important information is the dynamics of the pump unit which in the 1st design has resulted to be too slow because of the high thermal mass in contact with the heater. This observation has put into evidence the need of a new design with hanging heater. In this way is possible to isolate the heater from the rest of the package and to obtain very fast dynamics, as shown in the simulations. After this work, we have seen that with proper design of the micropump the thermal behaviour of the V-MCM need not to be a limiting factor even with the presence of high power dissipation.

ACKNOWLEDGEMENTS

We would like to thank the rest of the BARMINT partners for their collaboration: CNM, LAAS, TIMA, THD, TUL, TUB and to the UE for their funding.

REFERENCES

1. M. Carmona, S. Marco, H. Nguyen, U. Lundquist, A. Pardo, J. Samitier, A behavioural model for the dynamic simulation of micromachined thermo-pumps, Proc. 3rd Advanced Training Course on Mixed Design of Integrated Circuits and Systems, Lodz, Poland, June 1996, ed. A. Napieralski and M. Turowski, pp. 458-463.
2. M. Carmona, S. Marco, J. Samitier, J. R. Morante, Dynamic simulations of Micropump. Proc. Micro Mechanics Europe, Copenhagen, September 3-5, 1995, pp. 213-216.
3. G. Kelly, C. Lyden, C. O'Mathuna, J. S. Campbell; "Investigation of Thermomechanically Induced Stress in a PQFP 160 Using Finite Element Techniques", Proc. 42nd IEEE Electronic Components & Technology Conf., San Diego, May 18-20, 1992, pp. 467-472.
4. J. C. Lyke; "Packaging Technologies For Space Based Microsystems And Their Elements", in Microengineering Technology for Space Systems, Aerospace Report No. ATR-95 (8168)-2, 1995, pp. 131-180.
5. C.Val, M. Leroy, The 3D interconnection - Applications for mass memory and microprocessors, Proc. ISHM Conference, Orlando, Florida, 1991, pp. 62-68.
6. G. Kelly, J. Alderman, C. Lyden and J. Barrett; "Microsystem Packaging: Lessons From Conventional Low Cost IC Packaging", Proc. of MME 96, Barcelona, Spain, Oct. 1996, pp. 219-224
7. W. H. Ko, Packaging of microsensors, Microsystem Technologies' 94 4th Int. Conf. and Exhibition on Micro Electro, Opto Mechanical Systems and Components, Berlin, 1994, ed. H. Reichel and A Heuberger, (Berlin: Vde-Verlag GMBH), pp. 477-80.
8. "BARMINT - Basic Research for Microsystems Integration ", Edited by D. Esteve, ISBN 2-85428-465-8.
9. Z. Brzozka, H. A. J. Holterman, G. W. N. Honig, U. M. Verherk; "Enhanced Performance of Potassium CHEMFETs by The Optimisation of a Polysiloxane Membrane", Sensors and Actuators B, 18-19 (1994), pp. 38-41.
10. B. H. van der Shoot, S. Jeanneret, A. van der Berg, N. F. de Rooij; "A Modular Miniaturised Chemical Analysis System", Sensors and Actuators B, 13-14 (1993), pp. 66-70
11. X. P.M. Hall, "Strain measurements during thermal chamber cycling of leadless ceramic chip carriers soldered to printed boards" in *Proc. IEEE 1984 ECC*, pp. 107-116.
12. R. Darveaux, I. Turlik, L.T. Hwang, A. Reisman, "Thermal Stress Analysis of Multichip Package Design", *IEEE Trans. Comp. Hyb. Manuf.* 12, (1989) pp. 663-672.
13. B.S. Lall, B.M. Guenin, R.J. Molnar, "Methodology for Thermal Evaluation of Multichip Modules", *IEEE Trans. Comp, Pack. and Manuf. Tech. A* 18 (1995) pp. 758-764.
14. C. Cahill, A. Compagno, J. O'Donovan, O. Slattery, S.C. Ó Mathuna, J. Barret, I. Serthelon, C. Val, J.P. Tigneres, J. Stern, P. Ivey, M. Masgrangeas, A. Coello-Vera, *IEEE Trans.. Comp. Pack. Manuf. Tech. A*, (1995) 765-771.